



# Structural and Optical Properties of Graphene-ZnO Nanohybrid Thin Films Synthesized by Spray Pyrolysis

Zahraa M. Talib, Azhar I. Hassan\*, Jehan A. Saimon

Laser Science and Technology Branch, Department of Applied Sciences, University of Technology – Iraq

## Article information

### Article history:

Received: October, 10, 2021

Accepted: April, 07, 2022

Available online: September, 10, 2022

### Keywords:

ZnO,  
Graphene nanoplate,  
Nanohybrid film,  
Nanocomposite

### \*Corresponding Author:

Azhar I. Hassan  
[azhar.hassan@yahoo.com](mailto:azhar.hassan@yahoo.com)

## Abstract

Graphene-ZnO nanohybrid thin films were prepared by spray pyrolysis technique at 350 °C. Different graphene nanoplate concentrations of 0.1, 0.2, 0.3, 0.4, and 0.5 wt.% were used to deposit films on quartz substrates. The Structural and optical properties of the nanohybrid films have been investigated. X-ray diffraction XRD results show that the films have a hexagonal wurtzite polycrystalline structure and no secondary phases were observed. The structural parameters of crystallite size, dislocation density, and microstrain have indicated that the addition of graphene has a strong effect on the microstructure of zinc oxide films. Surface morphological analysis of the ZnO-graphene films reveals that the graphene content effectively modifies the morphologies and grain growth of the ZnO microstructure. It was also found from the optical properties that the maximum energy gap for pure ZnO films was 3.4 eV which decreases to 2.7 eV as the concentration of graphene increases to 0.5 wt.%. Results confirmed that graphene can be used as an efficient modifier for band gap engineering and the microstructure of ZnO thin films for enhanced photovoltaic applications.

DOI: [10.53293/jasn.2021.4349.1102](https://doi.org/10.53293/jasn.2021.4349.1102), Department of Applied Sciences, University of Technology  
This is an open access article under the CC BY 4.0 License.

## 1. Introduction

In the last two decades, novel nanostructures based on carbon allotropes, such as diamond-like carbon (DLC), multiwall, and single-wall carbon nanotubes (MWCNT & SWCNT), fullerene, and graphene, have attracted much attention due to their potential applications for advanced technologies. Among all the nanostructures, graphene has gained the highest attention due to its amazing characteristics, including extreme conductivity, very high carrier mobility, electromechanical stability, and large surface area. Gradually, graphene has developed as one of the most promising materials for photovoltaic applications, such as solar cells [1, 2], photodetectors [3–5], and light-emitting diodes (LED) [6, 7]. As one of the allotropes of carbon; structurally graphene atoms are coordinated in a single two-dimensional layer of carbon atoms ordered in a honeycomb lattice. The bond distance of carbon-carbon (C–C) in one layer of graphene is about 0.142 nm [8–10], and the  $sp^2$  hybridization of these bonds is responsible for the high stability of graphene nanostructure. The single carbon bonds are extremely strong and allocated in one plane while an empty orbital is formed out of the plane. Each carbon atom is bonded to three other carbon atoms, while the free fourth electron will be responsible for electronic conduction. Despite intense attention and remarkably fast development in the field of graphene-associated research, there is still a long way to go for widespread of graphene application. It is primarily a result of the difficulty of reliably producing samples of high

quality, particularly in a scalable fashion, and of controllable alteration the graphene band gap. Previous studies indicate that the fabrication of heterojunction based on semiconductors and the allotropes of carbon such as graphene is very effective in reducing surface recombination [11, 12]. It has been observed that the graphene layers could reduce the series resistance of the silicon-based solar cell through the passivation of surface dangling bonds [8, 9, 13]. Consequently, by combining the well-known optical characteristics of zinc oxide with the superior electronic transport graphene properties, UV-sensitivity, a hybrid optoelectronic device has been developed [9, 14–16]. These hybrid devices may gain an extraordinary responsivity, making them very well suitable for photodetector applications. With a reducing the bandgap of zinc oxide by incorporating graphene and with the wide light-harvesting ability of graphene, nanohybrids of these two materials could enhance visible light responsivity. Moreover, the folded three-dimensional nanostructure can also enhance the electron conductivity and separation of photogenerated charge carriers and thus the photoconductive behaviour may significantly improve [8, 17]. Combining the electrical and optical properties of graphene could open up new horizons for photonics and optoelectronic applications. Several applications using graphene as a promising candidate can be proposed, which may include photodetectors, light-emitting devices, touch screens, transparent electrodes, and ultrahigh-frequency devices [18, 19]. Recently, several publications have been focused on the synthesis of graphene-ZnO nanohybrid structures to improve the device performances for photovoltaic applications [20–26]. The aim of the current work is a synthesis of graphene-ZnO nanohybrid thin films by spray pyrolysis technique and systematically study their structure and optical properties. The influence of various graphene content as a 2D nanostructure on the morphology and microstructure will be investigated.

## 2. Experimental Work

Graphene-ZnO thin films were deposited on quartz substrate by spray pyrolysis. Spraying solution with ZnCl<sub>2</sub> (HIMEDIA zinc chloride 99.0 wt.%) to make Zinc Oxide thin films and then add graphene (Skyspring Nanomaterials, Inc, USA, thickness 6-8 nm, Carbon content 99.5 wt.%, with electrical conductivity 10<sup>7</sup> S.m<sup>-1</sup>) with various concentrations (0, 0.1, 0.2, 0.3, 0.4 and 0.5 wt.%). The graphene nanoplates were dispersed in 50 mL of distilled water by ultrasonication for about 1 h and then mixed with the ZnCl<sub>2</sub> solutions by a magnetic stirrer. The quartz substrates were cleaned by sonication in ethanol to eliminate any contaminations. The solution was deposited on a substrate heated at 350 °C and a solution flow rate of 4 ml/min. The distance between the nozzle end and the substrate was about 30cm. XRD diffractometer (XRD 6000, Shimadzu, Japan) with wavelength (1.5406 Å for CuKα) was used to analyze the phases and the crystalline structure. UV-VIS spectrophotometer (Shimadzu 3101 PC) was used to measure the spectral transmission of thin films. The surface morphology of deposited films was examined using the field emission scanning electron microscope FESEM model (Zeiss Sigma 300-HV Germany).

## 3. Results and Discussion

Figure 1 shows XRD patterns of ZnO and graphene-ZnO thin films deposited at 350 °C temperature and confirmed the ZnO phases of the hexagonal wurtzite structure. All the crystalline planes (100), (002), (101), (102), (110) and (103) of the zinc oxide were obvious, and (002) was the preferred orientation. The XRD patterns of graphene-ZnO nanohybrids were almost identical to those of pure ZnO films, where no additional phases were observed. On the other hand, the addition of graphene does not essentially modify the crystal orientations or result in variation in ZnO preferred orientations. However, no graphene diffraction peaks were identified in the thin film patterns, since the amounts of graphene were too small to identify using the XRD technique, and the yield of graphene diffraction intensity is much lower than the yield of zinc oxide diffraction intensity [17, 23, 27, 28]. The lattice constants *a* and *c* could be estimated based on (002) orientation and the *d*-spacing *d*<sub>hkl</sub> of graphene-ZnO nanostructure films are listed in Table 1. It could be noticed that for all films the *d*-spacing does not change whatever the level of graphene content. Such behaviour suggests that the graphene nanostructures are incorporated into the zinc oxide matrix and have played a significant role in modifying the characteristics of the as-deposited nanohybrid films. Moreover, the crystallites size was estimated for the nanohybrid thin films by the Scherrer equation [28]:

$$D = (0.94 \lambda) / (\beta \cos \theta) \quad (1)$$

Where  $\theta$  is the Bragg's angle,  $\lambda$  is the X-rays wavelength (1.5406 Å for CuKα) while  $\beta$  is the full width at half maximum FWHM. Results show that crystallite size was affected by the concentration of graphene. It is decrease as the graphene content increase, and this is the reason for the decrease in the X-ray peak with the increase in the

percentage of graphene. Furthermore, the microstrain ( $\epsilon$ ) and the dislocation density ( $\delta$ ) are also determined via the well-known formulas [18, 29, 30]:

$$\epsilon = (\beta \cos\theta)/4 \quad (2)$$

$$\delta = 1/D^2 \quad (3)$$

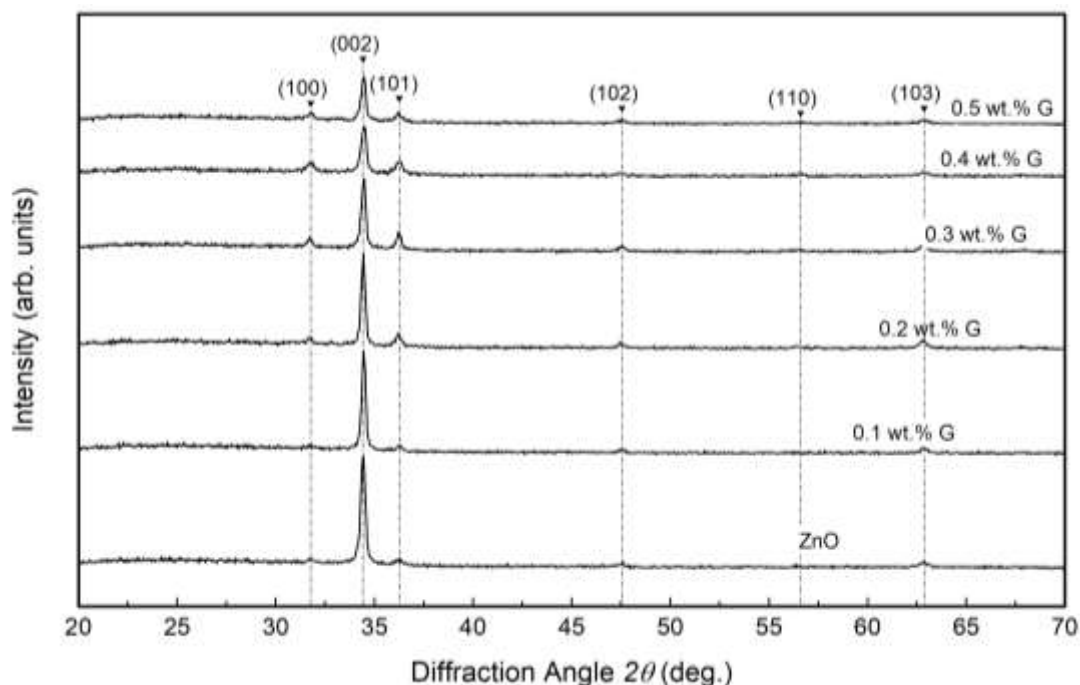


**Figure 1:** XRD pattern of ZnO-graphene thin films sprayed at 350 °C.

**Table 1:** The lattice parameters of graphene-ZnO thin films at different concentrations.

Sample	2θ (deg)	d (Å)	FWHM (deg)	D (nm)	$\delta \left( \frac{l}{nm^2} \right) \times 10^{-3}$	$\epsilon \times 10^{-3}$	a (Å)	c (Å)
ZnO	34.470	2.5998	0.2133	40.73	0.6027	0.888	3.0008	5.1976
0.1G	34.439	2.6021	0.2286	38.00	0.6924	0.952	3.0034	5.2021
0.2G	34.457	2.6007	0.2639	32.92	0.9226	1.099	3.0019	5.1995
0.3G	34.458	2.6007	0.2652	32.76	0.9317	1.105	3.0019	5.1994
0.4G	34.431	2.6027	0.2722	31.92	0.9817	1.134	3.0042	5.2034
0.5G	34.465	2.6002	0.3046	28.55	1.2271	1.268	3.0013	5.1985

The microstrain and density of dislocation were found to be increased with increasing the graphene content in the ZnO matrix. These constants are interesting structural parameters, and their values are crucial to understanding the electrical and optical behaviour of all graphene-ZnO nanohybrid films. In contrast to some reports in the literature [22], these findings have indicated that the addition of graphene has a strong effect on the microstructural feature of zinc oxide films. To investigate the influence of graphene content on the surface morphologies of the ZnO films, FESEM images were studied for all films as shown in Figure 2. The images showed that there are several morphological features were obtained on the films deposited under various graphene content. Zinc oxide film surface without graphene is covered with high packing hexagonal grains having a sharp crystal edge and narrow grain size distribution. With the addition of graphene as low as 0.1 wt.%, the zinc oxide crystals develop a finer grain with few grains that have to undergo an exaggerated growth, also the packing density of the grain has noticeably decreased. As the percentage of graphene was gradually increased, more random orientation of grains

has obtained with finer grain size. At a higher graphene content of 0.5 wt. %, graphene nanoplates nested with zinc oxide grains were observed.

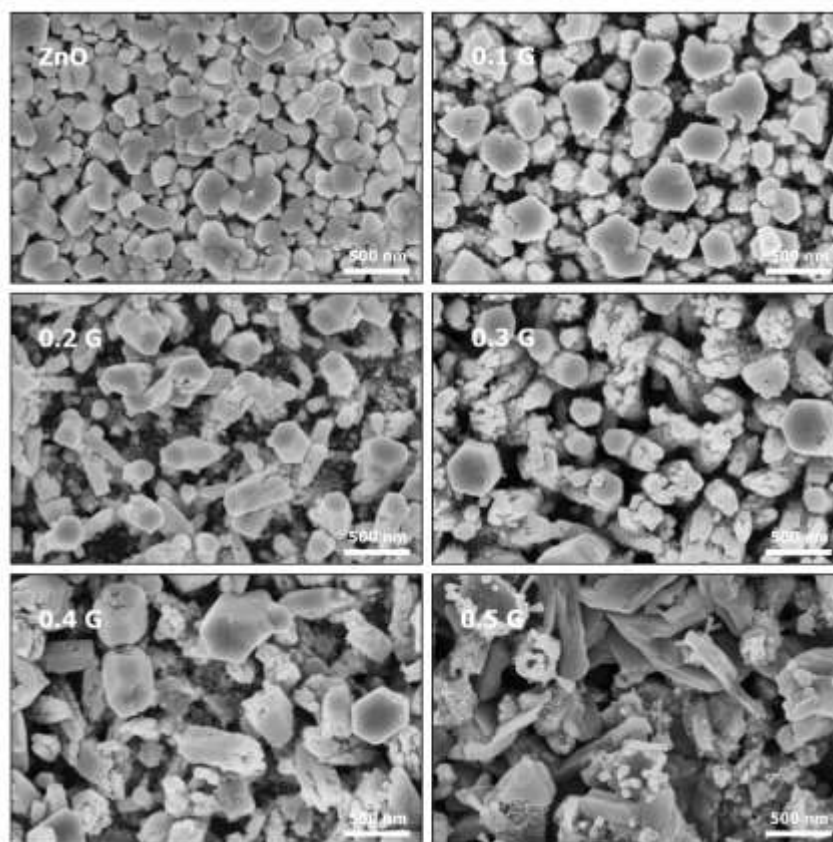


**Figure 2:** FESEM images of ZnO-G thin films morphologies with various graphene content.

Results suggest that the graphene nanoplate was strongly acted as grain growth inhibitors, which may explain the X-ray diffraction results of the films. As the size of the ZnO grains decreases, the total area of the grain boundaries increases and also the crystallite sizes decrease, thus increasing the structural defects and hence increasing the dislocation density. This was reflected in the decrease of the degree of crystallization of the films with adding more graphene nanoplates, which causes a decrease in the relative intensity of the diffraction patterns, as has been noticed with the most dominant plane (002). The transmission spectra analysis in the wavelength range (200-1100) nm can be revealed in Figure 3. According to the results, all films exhibit high transmittance in the visible range, varying between 80% and 90%. Also, the transmission of the ZnO film is found to be maximal and it reduces with a rise in graphene concentration. Figure 4 illustrates the absorption coefficient ( $\alpha$ ) values via wavelength which is deliberated via the equation [31]:

$$\alpha = \frac{1}{t} \ln \frac{1}{T} \quad (4)$$

Where  $t$  is the thickness of the thin film, and  $T$  is the transmittance. The figure confirms the decrease of absorption coefficient with wavelength and increases it with graphene concentration. While Figure 5 shows the extinction coefficient plot as a function of wavelength which appears the extinction coefficient increases with graphene concentration. The extinction coefficient values are calculated by the equation [32, 33]:

$$K = \frac{\alpha \lambda}{4\pi} \quad (5)$$



Using Tauc's plot, the optical band gap is gained by plotting  $(ahv)^2$  against  $(hv)$  as shown in Figure 6 and extrapolating the linear part of the curve to get the intercept with the energy axis. The direct energy band gap was decreased as the graphene concentration increased.

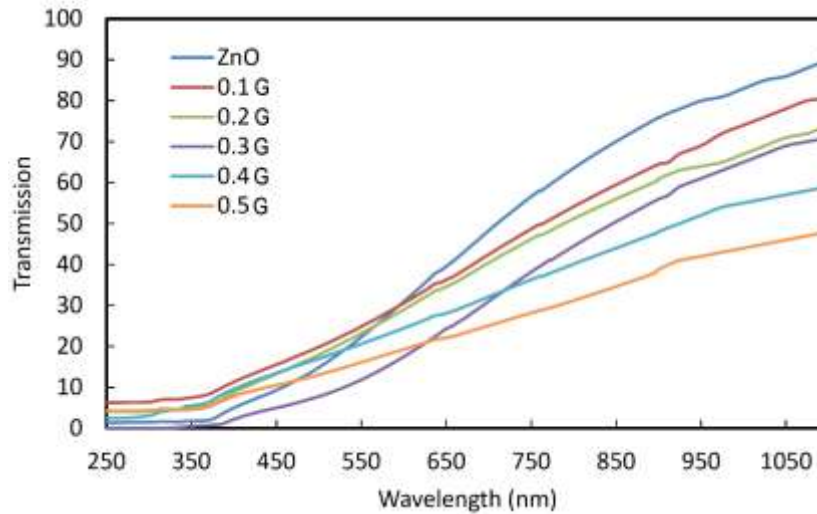


**Figure 3:** UV-Vis Transmission spectra of the nanohybrid graphene-ZnO thin films with different concentrations.

Graphene can decrease the band gap energy by removing the effect of Burstein-Moss also decreases the absorption edge of the nanohybrid thin films to the lower energies [12, 21]. Moreover, the presence of graphene in the films increases the surface charge and electronic coupling between ZnO grains and graphene nanoplatelets, which leads to a shift of the band gap towards the higher wavelengths, causing a narrowing of the band gap [16, 22]. Based on Figure 6, it is evident that the zinc oxide films have a single direct energy gap, while when graphene is added, two linear slopes have appeared and they became more distinct with increasing the graphene content. The findings support the presence of the nanohybrid system where the graphene and ZnO behave separately with the incident light, the data obtained, also, are highly consistent with the observed SEM images in the previous section. The determined direct energy gap for the films were 3, (2.9, 2.8), (2.6, 2.4), (2.7, 2.3), (2.5, 2), and (2.7, 2) eV to 0, 0.1, 0.2, 0.3, 0.4 and 0.5 wt.% graphene concentration, respectively. The decrease of the ZnO energy gap is ascribed to the internal defects rather than to the doping effect of carbon into the ZnO lattice, as has already been indicated by the high level of microstrain and dislocation density based on x-ray diffraction data presented in table 1.

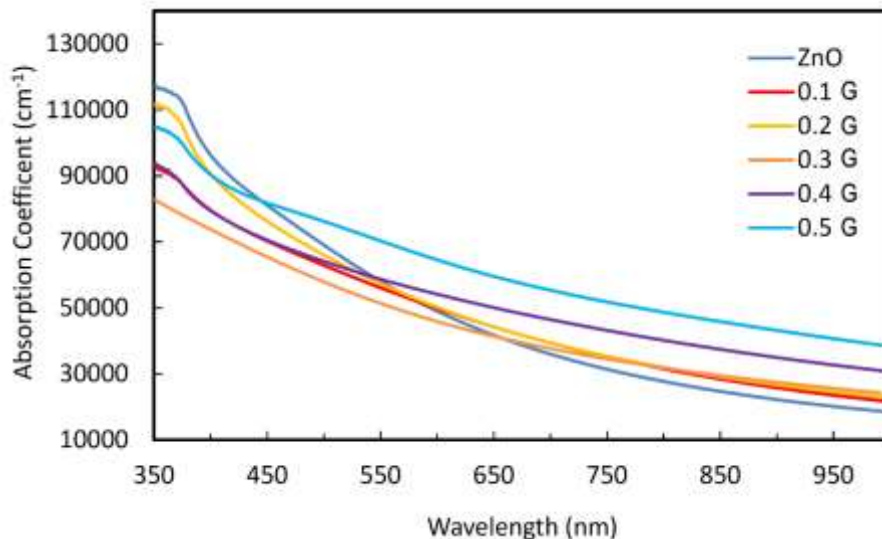


**Figure 4:** Absorption coefficient spectrum of the nanohybrid graphene-ZnO thin films at different concentrations.

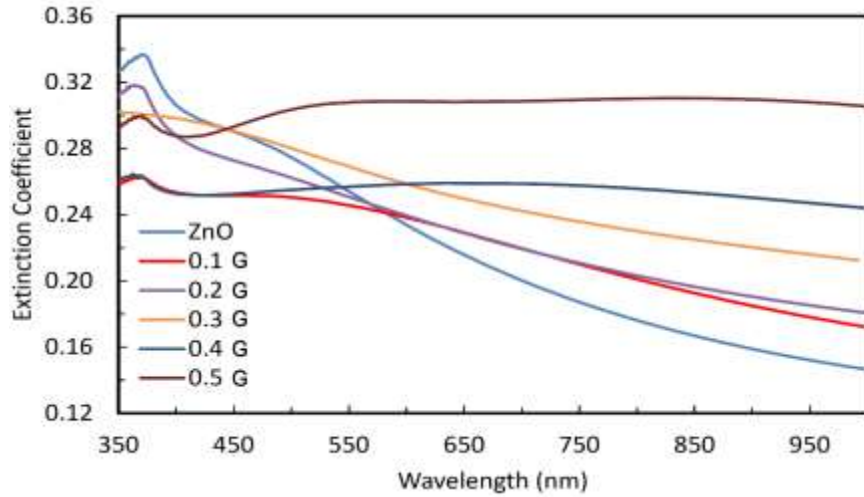


**Figure 5:** Extinction coefficient spectra of the nanohybrid graphene-ZnO thin films at different concentrations.

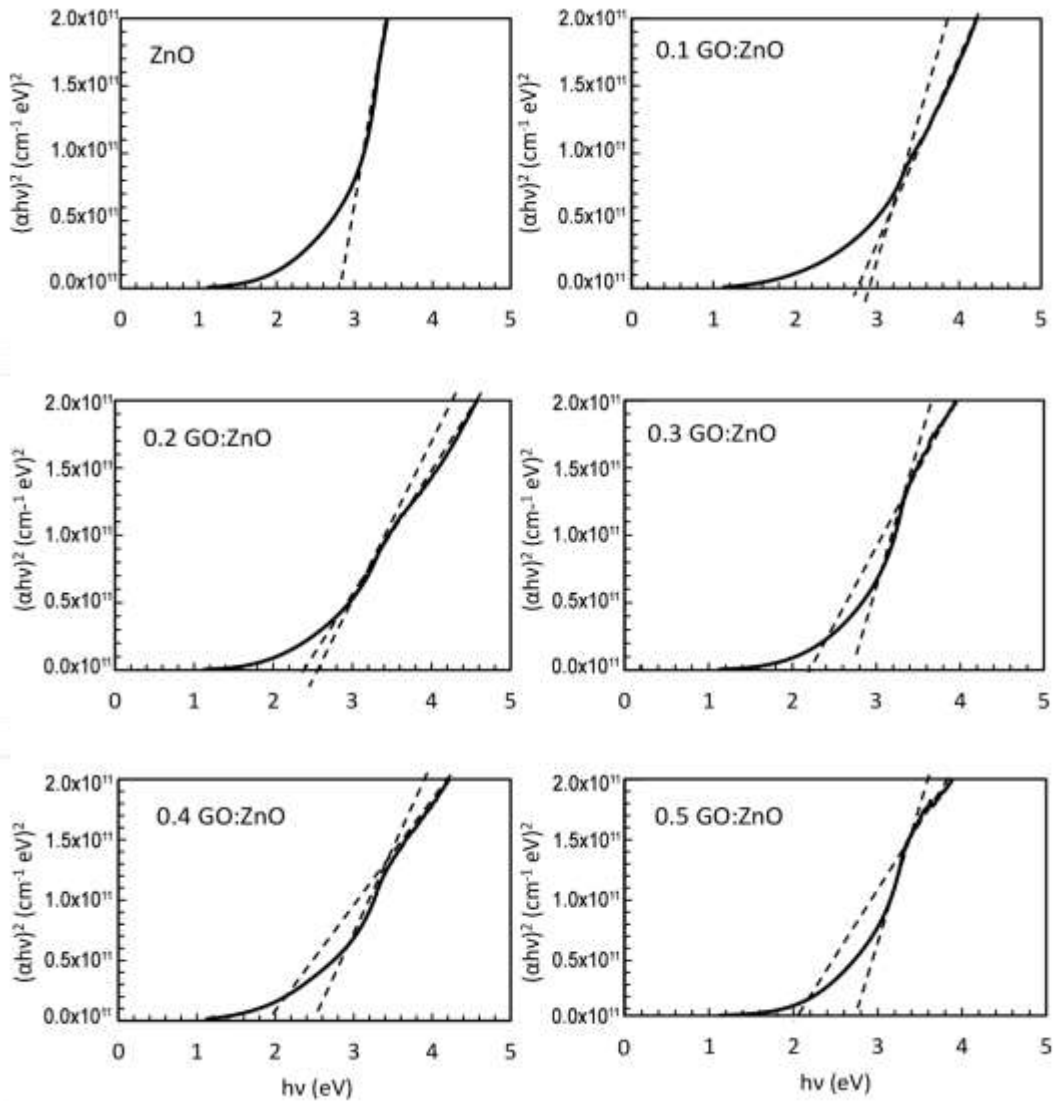


**Figure 6:** Plots of  $(ahv)^2$  versus  $(hv)$  of the nanohybrid graphene-ZnO thin films at different concentrations.

#### 4. Conclusions

In this work, graphene-ZnO nanohybrid thin films were effectively prepared using the spray pyrolysis technique at a substrate temperature of 350 °C. graphene-ZnO thin films possess a well-structured crystalline hexagonal wurtzite structure with a preferred orientation over the (002) orientation. The XRD analysis has also indicated that the addition of graphene has a strong effect on the microstructural feature of zinc oxide films. The presence of graphene in the microstructure of the ZnO films significantly affects the grains morphology and crystalline structure of the prepared films, where the graphene nanoplate act as grain growth inhibitors. The optical characteristics such as the transmission, optical band gap energy, and extinction coefficient were affected by graphene concentration in thin films. Results confirmed that graphene can be used as an efficient modifier for band gap engineering and the microstructure of ZnO thin films.

#### Acknowledgement

This work was conducted at the laboratories of Laser Science and Technology Branch, Applied Science Department, University of Technology, Baghdad, Iraq.

#### Conflict of Interest

The authors declare that they have no conflict of interest.

#### References

- [1] F. Gao, K. Liu, R. Cheng, and Y. Zhang, "Efficiency enhancement of perovskite solar cells based on graphene-CuInS<sub>2</sub> quantum dots composite: The roles for fast electron injection and light harvests," *Applied Surface Science*, vol. 528, p. 146560, 2020.
- [2] A. Das, S. R. Mondal, and G. Palai, "Realization of graphene based quantum dot solar cell through the principle of photonics," *Optik*, vol. 221, p. 165283, 2020.
- [3] K. Shimomura *et al.*, "Graphene photodetectors with asymmetric device structures on silicon chips," *Carbon Trends*, vol. 5, p. 100100, 2021.
- [4] H. Suo, S. Yang, P. Ji, and Y. Wang, "Multi-band enhanced graphene photodetector based on localized surface plasmon," *Sensors and Actuators, A: Physical*, vol. 322, p. 112627, 2021.
- [5] D. Chen *et al.*, "Self-powered ultraviolet photovoltaic photodetector based on graphene/ZnO heterostructure," *Applied Surface Science*, vol. 529, p. 147087, 2020.
- [6] S. H. Moon *et al.*, "van der Waals gap-inserted light-emitting p-n heterojunction of ZnO nanorods/graphene/p-GaN film," *Current Applied Physics*, vol. 20, no. 2, pp. 352–357, 2020.
- [7] Z. Wu *et al.*, "Ultra-stable phosphor of h-BN white graphene-loaded all-inorganic perovskite nanocrystals for white LEDs," *Journal of Luminescence*, vol. 219, p. 116941, 2020.
- [8] L. M. Malard, M. A. Pimenta, G. Dresselhaus, and M. S. Dresselhaus, "Raman spectroscopy in graphene," *Physics Reports*, vol. 473, no. 5–6, pp. 51–87, 2009.
- [9] L. A. Silva *et al.*, "Graphene as interface modifier in ITO and ITO-Cr electrodes," *Current Applied Physics*, vol. 20, no. 7, pp. 846–852, 2020.
- [10] A. AlShammari *et al.*, "The effect of substrate temperatures on the structural and conversion of thin films of reduced graphene oxide," *Physica B: Condensed Matter*, vol. 572, pp. 296–301, 2019.
- [11] A. S. AlShammari, M. M. Halim, F. K. Yam, and N. H. M. Kaus, "Effect of precursor concentration on the performance of UV photodetector using TiO<sub>2</sub>/reduced graphene oxide (rGO) nanocomposite," *Results in Physics*, vol. 19, 2020.
- [12] T. D. Nguyen-Phan *et al.*, "The role of graphene oxide content on the adsorption-enhanced photocatalysis of titanium dioxide/graphene oxide composites," *Chemical Engineering Journal*, vol. 170, no. 1, pp. 226–232, 2011.
- [13] V. Galstyan *et al.*, "Vertically aligned TiO<sub>2</sub> nanotubes on plastic substrates for flexible solar cells," *Small*, vol. 7, no. 17, pp. 2437–2442, 2011.

- [14] A. S. AlShammari, M. M. Halim, F. K. Yam, and N. H. M. Kaus, "Synthesis of Titanium Dioxide (TiO<sub>2</sub>)/Reduced Graphene Oxide (rGO) thin film composite by spray pyrolysis technique and its physical properties," *Materials Science in Semiconductor Processing*, vol. 116, p. 105140, 2020.
- [15] A. Janotti and C. G. Van De Walle, "Fundamentals of zinc oxide as a semiconductor," *Reports on Progress in Physics*, vol. 72, no. 12, 2009.
- [16] R. Paul, R. N. Gayen, S. Biswas, S. V. Bhat, and R. Bhunia, "Enhanced UV detection by transparent graphene oxide/ZnO composite thin films," *RSC Advances*, vol. 6, no. 66, pp. 61661–61672, 2016.
- [17] A. Galal, H. K. Hassan, N. F. Atta, A. M. Abdel-Mageed, and T. Jacob, "Synthesis, structural and morphological characterizations of nano-Ru-based perovskites/RGO composites," *Scientific Reports*, vol. 9, no. 1, pp. 1–13, 2019.
- [18] P. P. Sahay and R. K. Nath, "Al-doped ZnO thin films as methanol sensors," *Sensors and Actuators, B: Chemical*, vol. 134, no. 2, pp. 654–659, 2008.
- [19] V. Singh, D. Joung, L. Zhai, S. Das, S. I. Khondaker, and S. Seal, "Graphene based materials: Past, present and future," *Progress in Materials Science*, vol. 56, no. 8, pp. 1178–1271, 2011.
- [20] L. H. Liu, R. Métivier, S. Wang, and H. Wang, "Advanced nanohybrid materials: Surface modification and applications," *Journal of Nanomaterials*, vol. 2012, pp. 2012–2014, 2012.
- [21] B. Li, T. Liu, Y. Wang, and Z. Wang, "ZnO/graphene-oxide nanocomposite with remarkably enhanced visible-light-driven photocatalytic performance," *Journal of Colloid and Interface Science*, vol. 377, no. 1, pp. 114–121, 2012.
- [22] M. Karyouli *et al.*, "Physical properties of graphene oxide GO-doped ZnO thin films for optoelectronic application," *Applied Physics A: Materials Science and Processing*, vol. 127, no. 2, pp. 1–14, 2021.
- [23] H. Afzal *et al.*, "Enhanced drug efficiency of doped ZnO–GO (graphene oxide) nanocomposites, a new gateway in drug delivery systems (DDSs)," *Materials Research Express*, vol. 7, no. 1, p. 015405, 2020.
- [24] M. J. S. Spencer, "Gas sensing applications of 1D-nanostructured zinc oxide: Insights from density functional theory calculations," *Progress in Materials Science*, vol. 57, no. 3, pp. 437–486, 2012.
- [25] S. Sha *et al.*, "One-step electrodeposition of ZnO/graphene composite film as photoanode for dye-sensitized solar cells," *Colloids and Surfaces A: Physicochemical and Engineering Aspects*, vol. 630, p. 127491, 2021.
- [26] G. Khurana, S. Sahoo, S. K. Barik, and R. S. Katiyar, "Improved photovoltaic performance of dye sensitized solar cell using ZnO-graphene nano-composites," *Journal of Alloys and Compounds*, vol. 578, pp. 257–260, 2013.
- [27] X. Liu *et al.*, "UV-assisted photocatalytic synthesis of ZnO-reduced graphene oxide composites with enhanced photocatalytic activity in reduction of Cr(VI)," *Chemical Engineering Journal*, vol. 183, pp. 238–243, 2012.
- [28] S. J. S. Qazi, A. R. Rennie, J. K. Cockcroft, and M. Vickers, "Use of wide-angle X-ray diffraction to measure shape and size of dispersed colloidal particles," *Journal of Colloid and Interface Science*, vol. 338, no. 1, pp. 105–110, 2009.
- [29] Z. Khedaer, D. Ahmed, and S. Al-Jawad, "Investigation of Morphological, Optical, and Antibacterial Properties of Hybrid ZnO-MWCNT Prepared by Sol-gel," *Journal of Applied Sciences and Nanotechnology*, vol. 1, no. 2, pp. 66–77, 2021.
- [30] K. H. Aboud, N. Jamal Imran, and S. M. H. Al-Jawad, "Structural, Optical and Morphological Properties Cadmium Sulfide Thin Films Prepared by Hydrothermal Method," *Journal of Applied Sciences and Nanotechnology*, vol. 1, no. 2, pp. 49–57, 2021.
- [31] A. Hassan, K. Khashan, and S. Jehan, "Preparation and Characterization of NiO Thin Films by PLD," *Engineering and Technology Journal*, vol. 33, no. 1, 2014.
- [32] J. A. Saimon, D. S. Jbaier, and A. I. Hassan, "Influence of Annealing on Properties of Cadmium Oxide thin Films Prepared by Spray Pyrolysis," *Engineering and Technology Journal*, vol. 33, no. 8, pp. 1458–1466, 2015.



- [33] P. Norouzzadeh, K. Mabhouti, M. M. Golzan, and R. Naderali, "Investigation of structural, morphological and optical characteristics of Mn substituted Al-doped ZnO NPs: A Urbach energy and Kramers-Kronig study," *Optik*, vol. 204, p. 164227, 2020.